



Accuracy evolution and path compensation in 3D laser cutting process for advanced high strength steel parts: numerical analysis and experimental investigation

Rui Wang^{1,2,3,4} · Zhili Hu^{1,2,3,4} · Qiu Pang⁵ · Peng Liu⁶

Received: 22 August 2022 / Accepted: 17 December 2022 / Published online: 29 December 2022
© The Author(s), under exclusive licence to Springer-Verlag France SAS, part of Springer Nature 2022

Abstract

Advanced high strength steel (AHSS) has been widely used in automobile components due to its good lightweight effect and high safety. 3D laser cutting is the most dominant method for removing material from AHSS. However, the springback in the whole manufacturing process severely causes 3D laser cutting path deviations. To improve the cutting accuracy, a novel 3D laser cutting path compensation method considering the springback transfer is proposed in this paper. The AHSS A-pillar is used to investigate the springback behavior in the whole process. The hot stamping finite element model and 3D laser cutting finite element model are established, respectively. Through the finite element simulation analysis, the accuracy evolution law of the part during the whole process is discussed. Based on the accuracy evolution law of the hot stamping and the accuracy evolution law of the laser cutting process, the proposed compensation method is employed to modify the laser cutting path. The modified path is then applied to a 3D laser cutting experiment. The experimental results show that the deviation value is reduced by about 15% compared with the conventional 3D laser cutting process. The proposed 3D laser cutting path compensation method shows the advantage of high accuracy, which can also effectively improve production efficiency.

Keywords 3D laser cutting path · Path compensation · Springback · Advanced high strength steel (AHSS)

Introduction

In recent years, AHSS parts have been employed in automobiles, guaranteeing crash safety and meeting the development trend of lightweight [1, 2]. After the hot stamping process, 3D laser cutting technology is usually used to remove the workpiece material as the parts' strength usually reaches 1500 MPa. The 3D laser cutting is an advanced material cutting technology with the advantages of high accuracy, high speed, and small heat-affected zone. 3D laser cutting is usually influenced only by the melting point of the material and almost not by the strength. Therefore, as an essential process for processing AHSS parts, the accuracy of 3D laser cutting strongly affects the final accuracy of the part.

For the 3D laser cutting process, different parameters have different effects on 3D laser cutting accuracy. Many kinds of research have been conducted around process parameter design and optimization. Miraoui et al. [3] studied the effect of process parameters on the melting zone depth

✉ Zhili Hu
zhilihuhit@163.com

✉ Qiu Pang
pqiu@wust.edu.cn

¹ Hubei Key Laboratory of Advanced Technology for Automotive Components, Wuhan University of Technology, Wuhan 430070, China

² Hubei Longzhong Laboratory, Xiangyang 441000, Hubei, China

³ Hubei Research Center for New Energy & Intelligent Connected Vehicle, Wuhan University of Technology, Wuhan 430070, China

⁴ Hubei Engineering Research Center for Green & Precision Material Forming, Wuhan University of Technology, Wuhan 430070, China

⁵ School of Machinery and Automation, Wuhan University of Science and Technology, Wuhan 430081, China

⁶ Dongfeng (Wuhan) Industrial Co., Ltd., Wuhan 430040, China

and heat-affected zone depth. It was found that increasing the laser cutting speed, decreasing the laser power, and laser beam diameter can reduce the melting zone depth and heat-affected zone depth. Russo et al. [4] found that the laser cutting speed has the most significant influence on the cutting quality of hot-stamped boron steel sheets. In order to obtain better process parameters, some advanced optimization methods have been employed in many previous kinds of research. The process parameters for laser cutting of composite laminates were optimized based on the response surface methodology [5]. The response surface methodology can also be adopted to develop mathematical models for geometrical quality characteristics [6]. Compared to Taguchi's method, Nguyen et al. [7] found that the response surface method has better elucidation of the interaction effects of each process parameter. Madić et al. [8] used the exhaustive iterative search algorithm to achieve the optimization of laser cutting parameters.

Many literatures also focus on the quality of the laser cutting kerf, such as roughness, slag size, etc. For kerf quality, Shrivastava et al. [9] investigated the effect of cutting parameters on top kerf width and bottom kerf width using the response surface method, and the genetic algorithm was employed to optimize the response surface model. Based on this, Girdu et al. [10] also used this approach to obtain more specific cutting parameters such as laser cutting power, the pressure of the auxiliary gas, and cutting speed to obtain higher quality cuts. As for roughness, the literature [11–14] have studied the effect of laser cutting process parameters on the surface roughness of the workpiece. Many literatures also reported the law of the influence of process parameters on the size of floating slag during laser cutting and some relevant prediction models based on some intelligent algorithms have been proposed [15–17]. Many scholars have also studied cutting efficiency based on satisfying the cutting accuracy. Shin et al. [18] developed a new cutting head with a longer focal length to achieve high-speed cutting of thick steel plates. Oh et al. [19] found that supersonic laser cutting not only allows for more considerable cutting distances, but also increases efficiency. Rodrigues et al. [20] investigated the maximum cutting speed achieved for a given plate thickness. Based on this, Shin et al. [21] found that the cutting speed could be further increased by tilting the cutting head by 15°.

From the above literature, it is clear that optimizing the laser cutting process parameters can improve the forming quality of the cut part, guarantee the forming accuracy and improve the cutting efficiency. However, in the actual processing and production process, the contour accuracy of the workpiece is still not high, and the commissioning period is extended. Probably, this is due to the errors in the dimensions of the workpiece itself when it is cut by the laser. One of the primary sources of errors occurring in the workpiece

is springback. The springback occurs mainly in two aspects: the first one is the springback generated after hot stamping [22–27]. The second one is that the laser cutting clamps cause elastic deformation of the workpiece, causing dimensional errors that reduce laser cutting accuracy. Li et al. [28] found that the positioning accuracy of the workpiece could be improved by optimizing the clamping force of the fixture. Abedini et al. [29] used a genetic algorithm to optimize the clamping layout to improve positioning accuracy. As reported in the literature [30, 31], especially for thin-walled components with low stiffness, the fixture undergoes large elastic deformation during clamping. Therefore, the clamping of the fixture during laser cutting resulting in off-setting of the workpiece from cut's original position, cannot be ignored. Huang et al. [32] proposed a two-dimensional contour compensation system, in which a non-contact sensor is used to detect errors. After compensation, the contour accuracy is improved by 80% at high feed rates.

Due to the unloading of forming force, clamping, and other factors, the workpiece will produce unavoidable springback. The springback leads to long commissioning cycles, low accuracy, low efficiency, and high cost in stamping or laser cutting processes. Figure 1 shows the main forming processes of the AHSS part. After the hot stamping process, if the 3D laser cutting path is executed according to the original path, the contour profile or the holes will produce specific errors. These errors directly affect the cutting accuracy of parts. Hence, the compensation of the 3D laser cutting path for springback parts is significant.

In this paper, a new method, a 3D laser cutting single path compensation method considering springback transfer, is proposed. The remainder of this paper is organized as follows. In Section "[3D laser cutting path compensation method considering springback transfer](#)", The motivation for proposing this method is clarified, and the specific compensation of this new method is presented. In Section "[Experimental and numerical simulation](#)", numerical simulations and experiments of hot stamping and laser cutting are done. The compensation of the path based on the new method is performed and verified by experiments. In Section "[Conclusions](#)", the main findings of the research work are concluded.

3D laser cutting path compensation method considering springback transfer

3D laser cutting is the last process in the hot stamping line for AHSS. The numerical simulation should fully consider the impact of the previous process on the workpiece. The whole numerical simulation process should include sheet stamping, die unloading, hole cutting, trimming, and other processes. The state of the workpiece after stamping and unloading is the initial state of the 3D laser cutting and

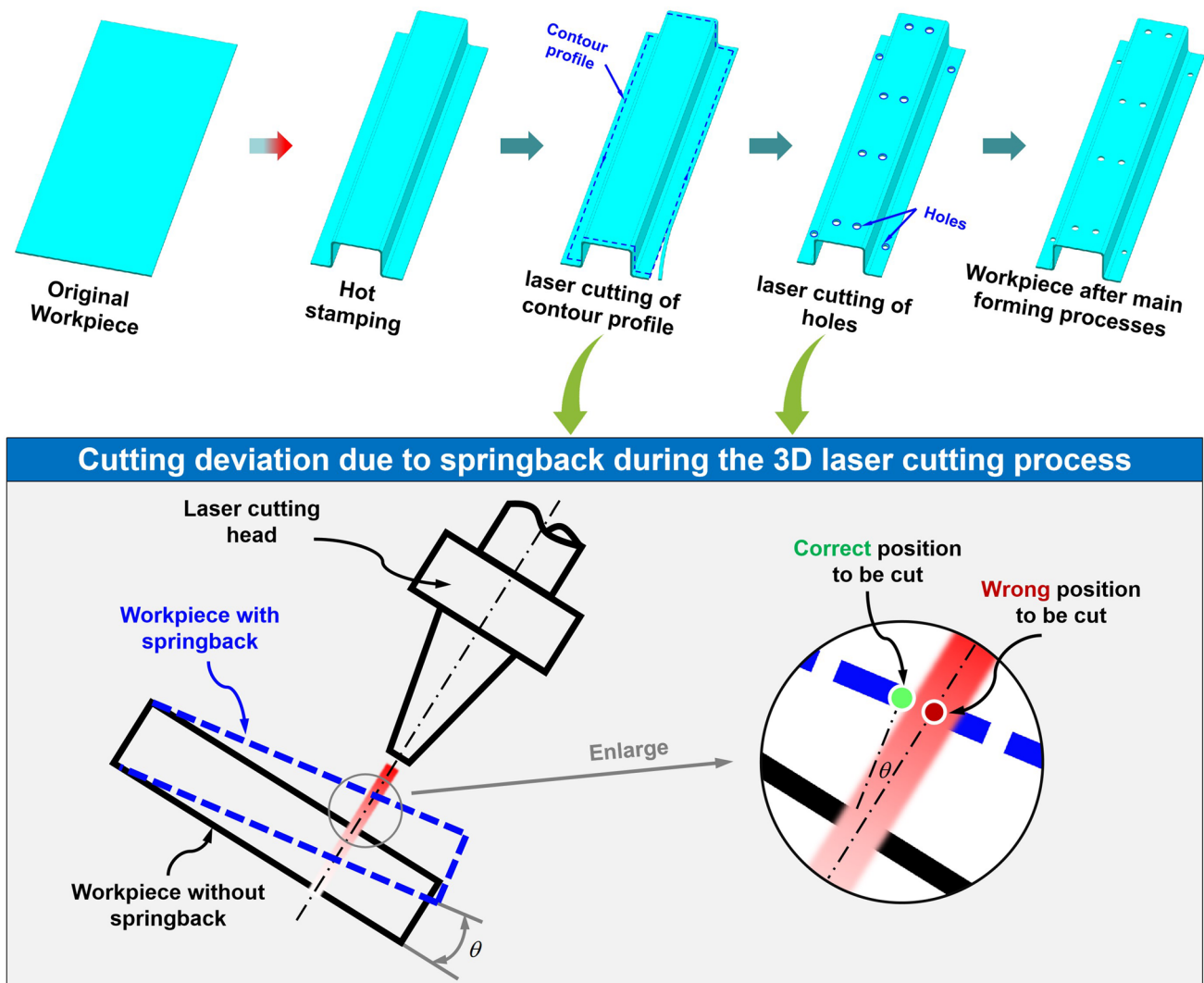


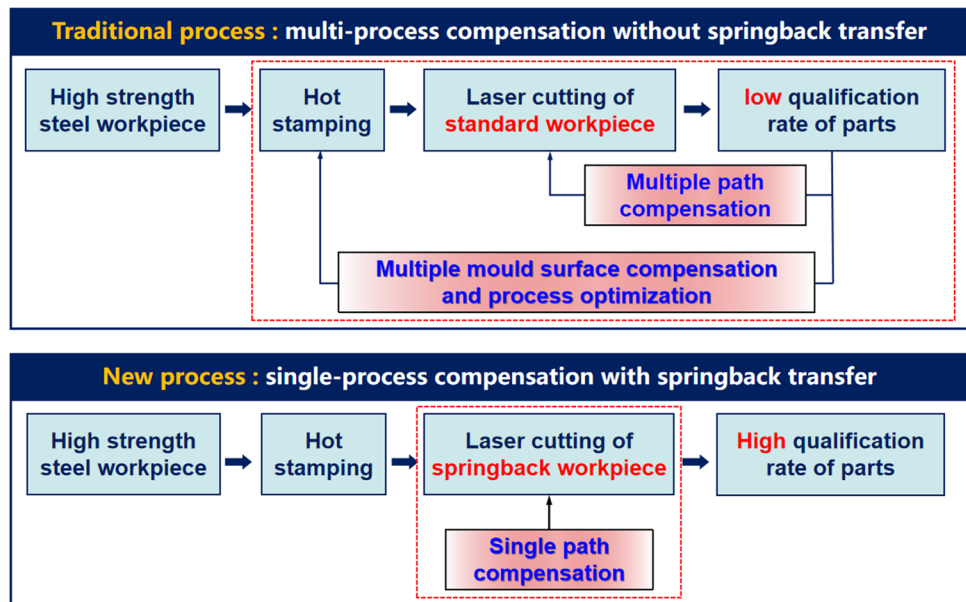
Fig. 1 3D Laser cutting deviations in the whole manufacturing processes of AHSS part

trimming. 3D laser cutting is an orderly time-sharing process, and each section's cutting result will impact the cutting accuracy of the subsequent section. In the production process, the clamps will be closed sequentially according to the cutting order to ensure that there will be no interference with the cutting head while ensuring the clamping of the workpiece. In summary, the two major contributors to deviations in the laser cutting path are the springback of the workpiece after hot stamping and the springback caused by the clamping of the laser cutting clamps. The existing studies on springback compensation for AHSS parts usually focus on one process. The transfer of rebound between the main processes is not traditionally considered. That results in the need to repeatedly adjust the parameters of the stamping process or the 3D laser cutting process.

Figure 2 shows a process comparison between conventional springback compensation and novel springback

compensation for the AHSS part. In the traditional process, an AHSS workpiece is hot stamped to form an intermediate part. The intermediate part is cooled and sent to a laser cutting platform where holes and contours will be cut. To reduce the impact of springback on forming accuracy, multiple path compensations for laser cutting or multiple die face compensations and process optimization in the hot stamping process are usually required. This constant commissioning leads to high costs and low efficiency. We found that the reason for the above problem is mainly because the springback of the previous process is not considered to affect the subsequent process. Firstly, the clamp is also designed by the standard numerical model, and clamping will lead to elastic deformation of the workpiece and then affect the cutting path. Secondly, the cutting path is also designed by the standard numerical model, and there is deviation when cutting the workpiece with springback. Therefore, we propose a

Fig. 2 Comparison of traditional process and new process



laser cutting path compensation process considering springback transfer. This process can reduce the number of laser cutting commissioning, improve the cutting accuracy, and obtain parts with a higher qualification rate.

How to compensate for the cutting path is an urgent problem to be solved. Figure 3 shows the diagram of the springback of 3D laser cutting. The springback value in the XY plane affects the cutting contour, the springback in the Z direction affects the profile, and the characteristic point A is the point on the original laser-cut standard workpiece. In fact, due to the springback, the position of the cut point becomes A'. Then for the coordinates of the feature point A, the values to be compensated in the 3D coordinates are: Δx , Δy and Δz . The HSHSS parts are usually complex, and the rebound value of each point cannot be obtained accurately. Numerical simulation is used to obtain the rebound values for each segment of the cutting path at the feature

points in three directions. Based on the springback values, the 3D coordinates of each feature point are compensated. The compensation values are imported into the path generation CNC software to generate a new path. The new path is subsequently used to cut the workpiece, thereby improving the accuracy of the laser cutting.

Experimental and numerical simulation

Material and structure of part

The hot stamping structural part of AHSS used in this work is an A-pillar of a specific type of automobile. The material is 22MnB5, and its chemical composition is shown in Table 1. The data of chemical composition for 22MnB5 are from Baoshan Iron & Steel Co.,Ltd, which have been

Fig.3 The springback in 3D laser cutting

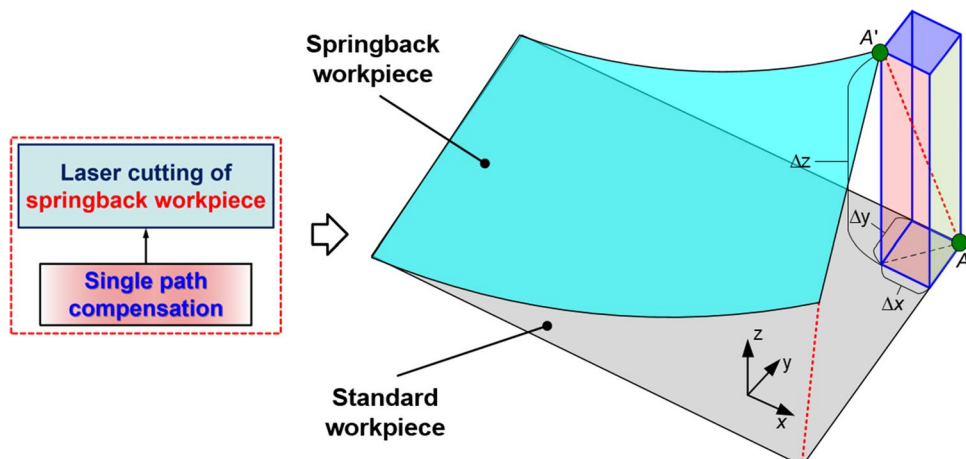


Table 1 The main chemical composition of 22MnB5 (mass fraction, %)

Ceq	C	Mn	Si	P	S	Al	Cr	B	Ti	N
0.55	0.25	1.7	0.4	0.03	0.01	0.06	0.5	0.055	0.05	0.009

Table 2 The mechanical properties of 22MnB5

Parameter	Yield strength/MPa	Tensile strength/MPa
After hot forming	1100	1475

tested and verified. The mechanical properties are shown in Table 2. The geometric model of the A-pillar structure is shown in Fig. 4. The thickness is 1.4 mm, the part length is 1237 mm, the width is 325 mm, and the height is 176 mm. The 3D laser cutting outline length is 4262 mm. The tolerance requirement of the part is also shown in Fig. 4.

3D laser cutting machine

The 3D laser cutting machine used in the experiment is the 3D laser cutting machine produced by Prima, Italy. The machine type is Laser Next LN1530-3D, and the laser type is IPG YLS-3000, as shown in Fig. 5. During the cutting process, the six clamps are closed and opened sequentially to avoid interference with the cutting head and complete each structure's cutting (e.g., holes, edges, etc.) smoothly. The main cutting parameters during the cutting process are laser power 2800 W, cutting speed 16 m/min, auxiliary gas pressure 12 bar, and frequency 1000 Hz.

Numerical simulation of springback

Finite element model of hot stamping

The hot stamping finite element model of the A-pillar was established by Autoform R7 sheet forming finite element software. Currently, Autoform R7 is more widely available commercially, making it easy to use the techniques in this paper for production trials. The 3D model of the part was expanded in the software to obtain a preliminary sheet. The sheet was set as an elastoplastic body, the material was set as 22MnB5, which comes with the software, the thickness was 1.4 mm, and the temperature was set to 930 °C. The upper and lower molds are set as rigid bodies, and the upper

and lower mold temperatures are set to 85 °C. The grid element division function that comes with the software is used to establish the blank element grid. The maximum element angle is 22.5°, the maximum element size is 40 mm, and the element type is EPS-11. The holding time is set to 8 s, the friction coefficient between the mold and the sheet is set to 0.45, and the stamping speed is set to 1500 mm/s. In order to prevent the sheet from shifting during the stamping process, positioning pins are placed according to the actual processing requirements. The established finite element model of hot stamping is shown in Fig. 6.

3D laser cutting finite element model

The laser cutting process can be seen as a rapid movement of the heat source over the surface of the workpiece. The laser heat source is loaded onto the workpiece surface and moves forward in the cutting direction. The laser heat source model is chosen as a semi-ellipsoidal heat source, and the heat flow density expression of the heat source model is:

$$q = \frac{6\sqrt{3P}}{abc\pi\sqrt{\pi}} \times e \left[-3\left(\frac{z-vt}{a}\right)^2 - 3\left(\frac{x}{b}\right)^2 - 3\left(\frac{y}{c}\right)^2 \right] \quad (1)$$

where P is the three-dimensional laser cutting power, W; v is the cutting speed, m/s; a, b and c are the heat source model parameters m. The values of each parameter are P=2800 W, v=0.26 m/s, and the spot radius is 0.0001 m.

The literature presented in the introduction shows that the laser cutting heat source has a negligible influence on the deformation at the kerf with the optimized process parameters. Significantly, the trimming tool in the Autoform software is approximated as a laser cutting beam to ensure the continuity of the multi-step simulation and the accuracy transfer effect.

To ensure the accuracy of the 3D laser cutting springback simulation, the simulation is calculated according to the cutting sequence of the actual 3D laser cutting. The cutting process is mainly divided into the removal of the material inside the sheet (holes) and the removal of the material outside the

Fig. 4 3D model of A-pillar with tolerance requirements

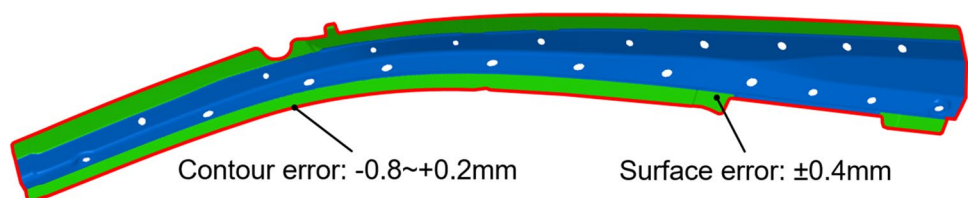


Fig. 5 3D laser cutting platform

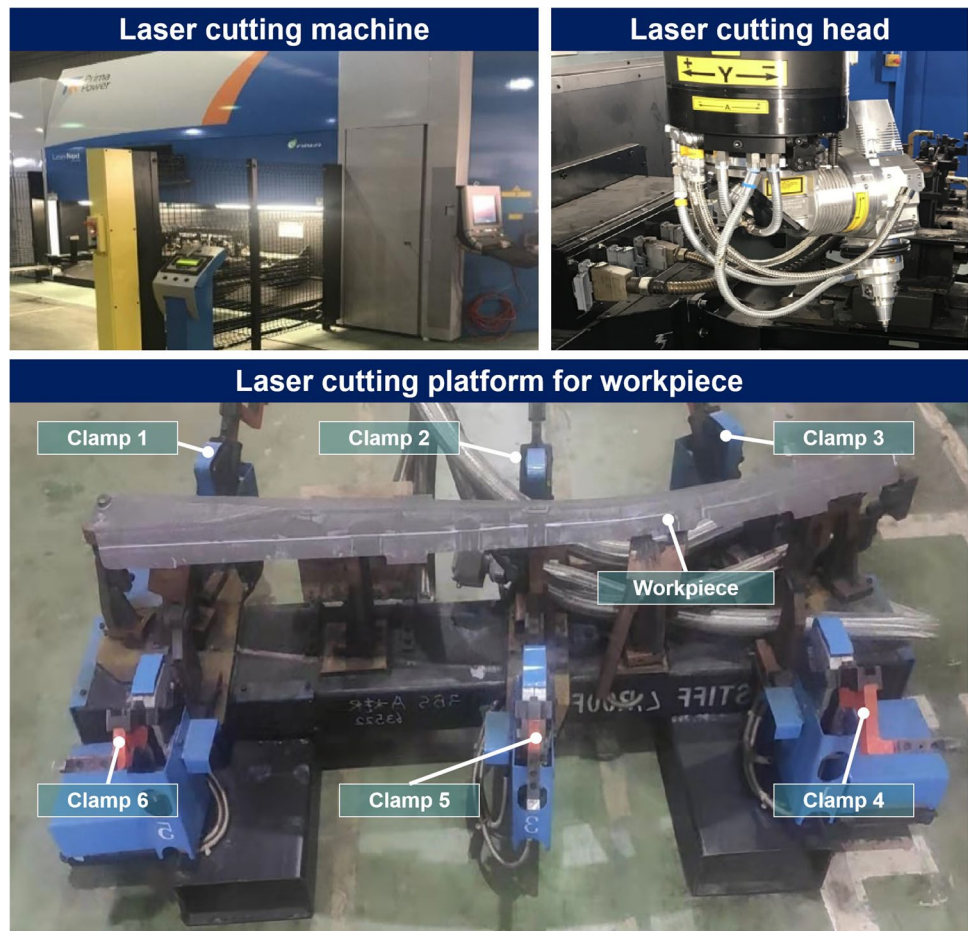
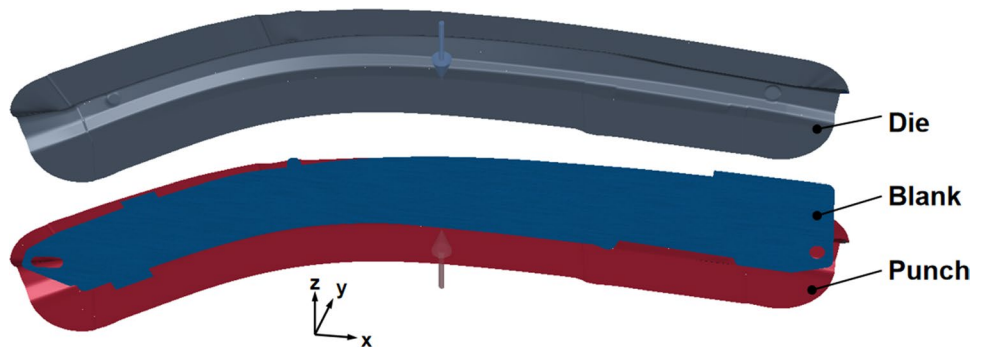


Fig. 6 Hot stamping FE model of AHSS A-pillar



sheet (contours). In the actual manufacturing process, the outer contour is segmented according to the processing order and the clamping of the clamps to trim the outer contour. Due to the clamping action of the clamps involved in the cutting process, there is more springback when cutting contours and relatively little when cutting holes. Consequently, the order of cutting holes can be placed either before or after the cutting contour. In order to simplify the numerical simulation process and reduce the influence of errors, the order of cutting holes is placed after cutting contour during the numerical simulation in this paper. Among them,

The springback calculation is carried out sequentially in the processing order. The cutting sequence and cutting contour are shown in Fig. 7.

Result and discussion

As shown in Fig. 8, the springback transfer law of the part during hot press forming, laser cutting trimming, and hole cutting is investigated by taking four sections of the A-pillar part. Ten feature points are taken from each section, and 40

Fig. 7 Cutting sequence and cutting contour

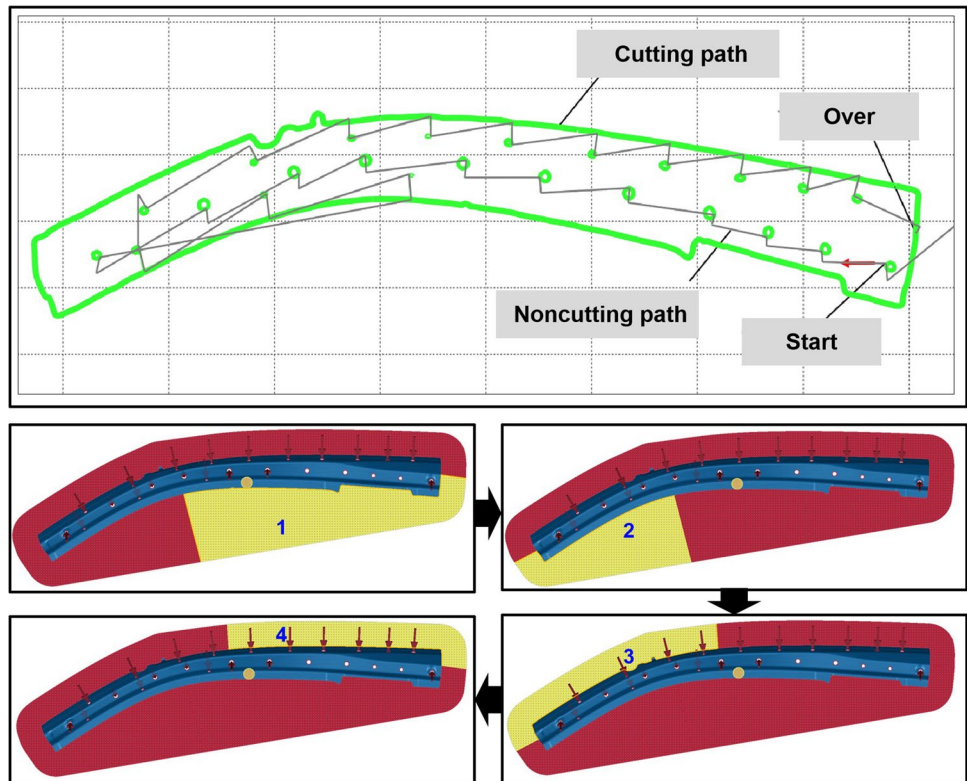
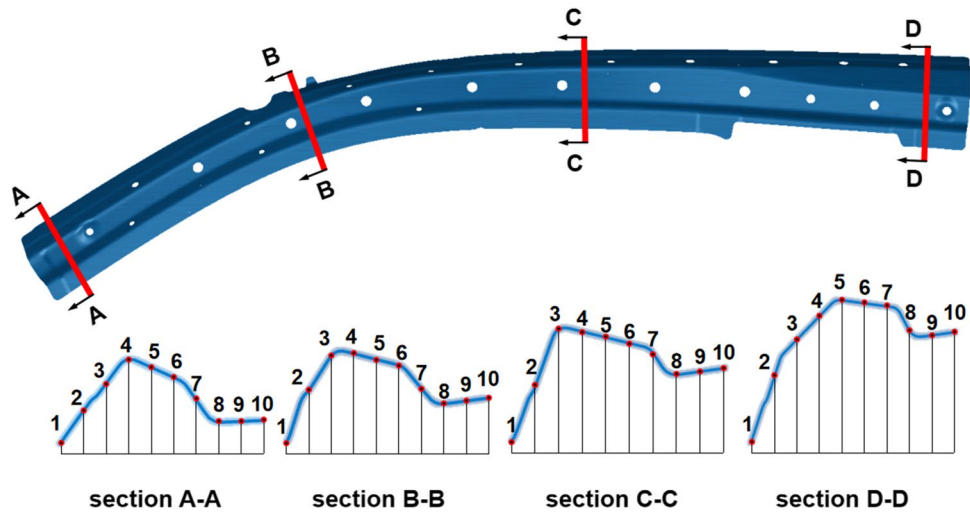


Fig. 8 Tracking points on sections



uniformly arranged feature points are taken from the whole part. In the software, the position of the feature points can be changed with the forming process, which can realize the function of springback tracking in the whole process.

Springback law for hot stamping process

After the blank is heated to stamping temperature, it is transferred by a robot to a press for forming. After the forming is completed, springback usually occurs, i.e., a difference

between the stamped and ideal stamped parts' dimensions. When the dimensional deviation caused by springback is too large, it is necessary to adjust the stamping process's parameters or modify the tool. When the dimensional deviation due to springback is within the tolerance range, the previous stamping process is not considered, and the part is moved to the following cutting process. In this case, the actual workpiece to be cut is the one that has been springbacked, not the theoretical one. In addition, the clamps on the laser cutting platform can also cause the workpiece to deform.

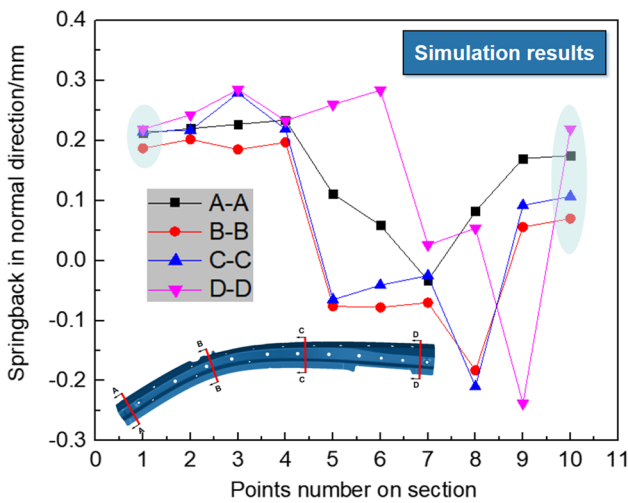


Fig. 9 Normal springback of stamping process

During the cutting process, multiple clamps close and open in sequence, causing the entire force on the workpiece to change. The force state is changed in real-time. Since the path of laser cutting is usually programmed according to the contour and holes on the standard model, there is a big difference between this ideal path and the actual path. The dimensional accuracy of the final cut finished part is not satisfactory, leading to constant cutting process debugging.

Therefore, the springback transfer law is first obtained after stamping, and the cut trim punching model is subsequently modified according to the springback law. The springback results of the stamping process are shown in Fig. 9. These results are from numerical simulations. The springback of the stamping process body structure member grows transversely from the center to both ends. Longitudinally, it increases from the center line of the body structure to both sides. However, although these errors impact the subsequent laser cutting process, they are within the tolerances required by the hot stamping process. Consequently,

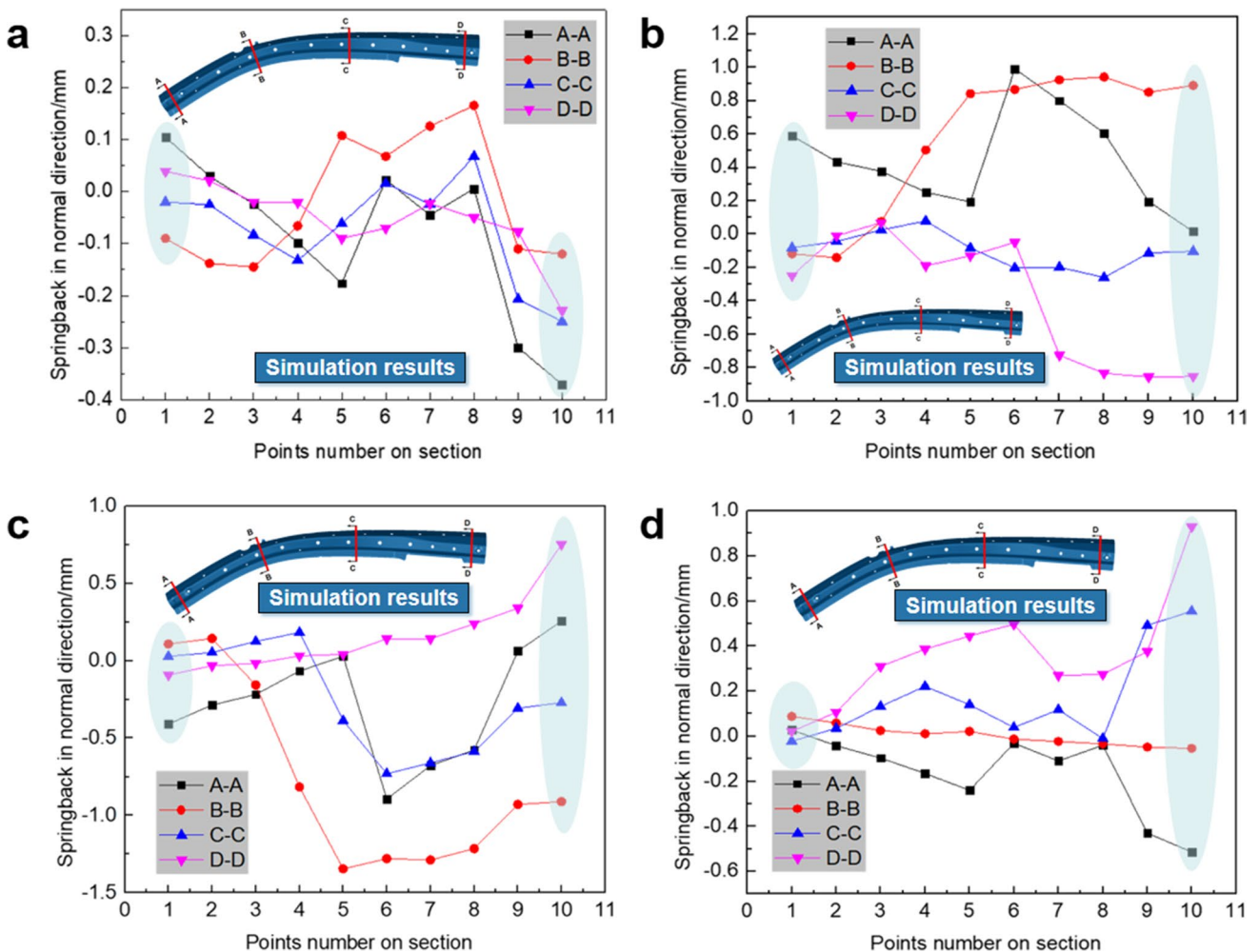


Fig. 10 Springback in the cutting process from step 1 to step 4

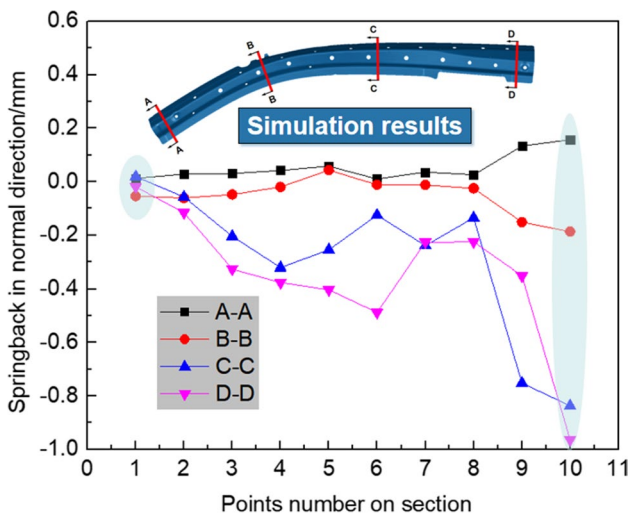


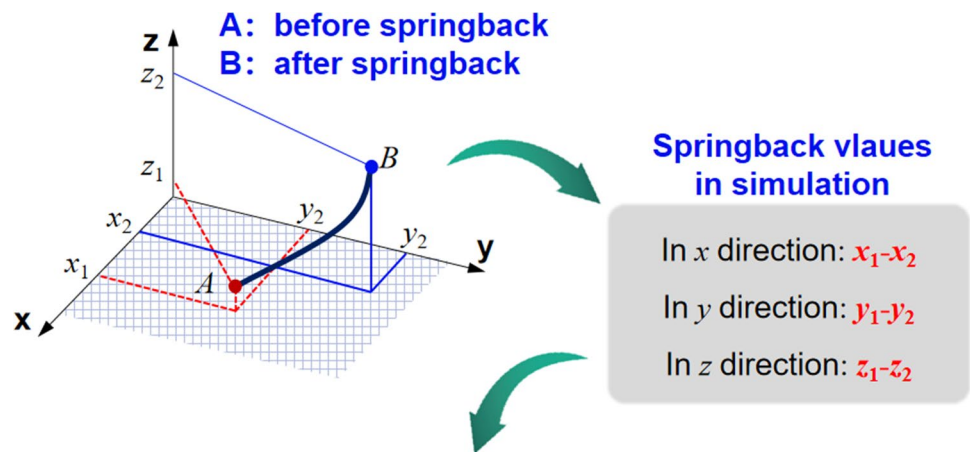
Fig. 11 Springback distribution during laser cutting holes

the subsequent process analysis can be performed in the finite element process.

Springback law for 3D laser cutting process

During the 3D laser cutting process, the laser cutting head cuts the workpiece along a programmed path. The clamps

Fig. 12 Compensation process in combination with numerical results



Modify the coordinate values on the cutting path

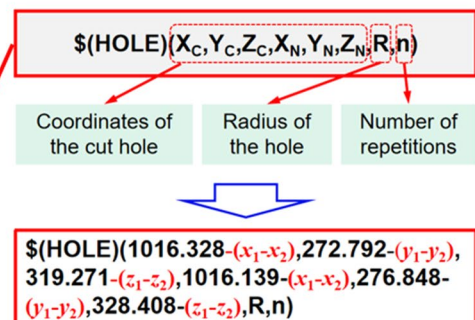
```

*END HEADER
G01 X1100.076 Y307.309 Z650 A186.403 B36.119
G01 X1100.076 Y307.309 Z338.767 A186.403 B36.119

!* START OF CIRCLE.1
$[APPROACH_MC] (1102.048, 289.735, 314.533, 186.403, 36.119)
$[WORK_ON](1)
$[HOLE] (1103.973, 292.174, 312.921, 1103.316, 298.032, 320.999, 5.48, 2)
$[WORK_OFF](1)
G09
F207000
$[RETRACT_MC] (1098.976, 305.915, 339.688, 186.403, 36.119)
G01 X1012.826 Y286.678 Z345.863 A182.663 B23.955

!* START OF CIRCLE.2
$[APPROACH_MC] (1013.392, 274.51, 318.448, 182.663, 23.955)
$[WORK_ON](1)
$[HOLE] (1016.328, 272.792, 319.271, 1016.139, 276.848, 328.409, 5.5, 2)
$[WORK_OFF](1)
G09
F207000
$[RETRACT_MC] (1011.148, 287.66, 345.393, 182.663, 23.955)
G01 X937.652 Y269.038 Z351.306 A186.654 B23.355
    
```

Path code



will open and close sequentially to avoid interference with the laser cutting head. At this time, each clamp clamping and unclamping will lead to errors in the 3D laser cutting process because of the springback in the previous process. The outer contour cutting process of the workpiece is divided into four zones 1,2,3 and 4 (see Fig. 7). The cutting process is carried out smoothly according to the four zones. When cutting area 1, the clamps in area 1 will be opened, and the clamps in other zones will remain clamped.

Springback during contour step cutting

The A-pillar structure is complex and has a particular curvature, and each section has a different shape. Thus, each zone of the part has a different extent of deformation. Conventional laser cutting simulations usually do not consider the effect of clamping conditions on cutting accuracy. In this paper, the idea of step-by-step cutting is proposed to investigate the springback during laser cutting. As shown in the cutting platform in Fig. 5, there are six clamps in total. In the cutting process, it usually appears that one clamp is opened when five clamps are clamped, or two clamps are opened when four clamps are clamped.

Figure 10a shows the step-by-step diagram of the springback of the part during the cutting of the edge in the first step. The results in Fig. 10a are from numerical simulations.

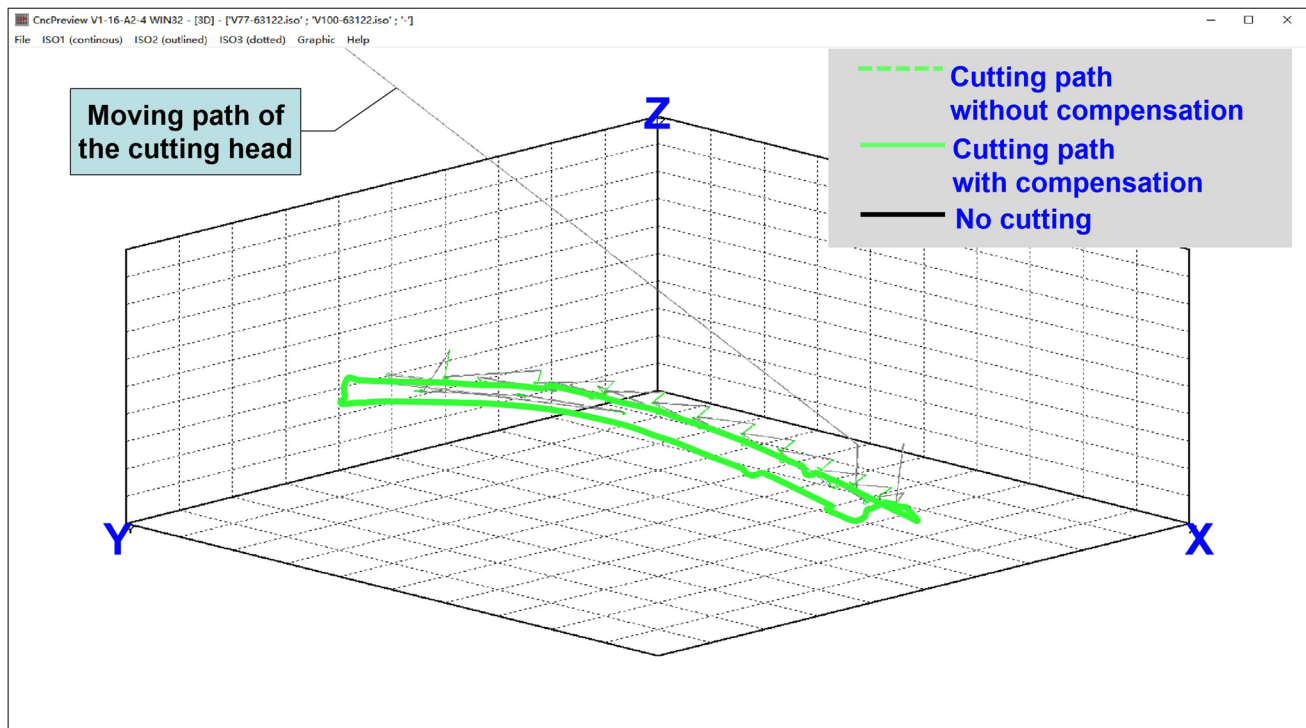


Fig. 13 3D cutting path diagram

At this point, clamps 1 and 2 are in the unclamped state and clamps 3, 4, 5, and 6 are in the clamped state. The feature points 1 and 10 on each cross-section represent the feature values on the contour, respectively. Sections A-A and D-D evolve from positive springback to negative springback. The changes in cross-sections B-B and C-C are relatively smooth. This indicates the torsional rebound of the workpiece due to the residual stress. The cutting trajectory of this section is compensated by the reverse of the rebound value of the feature point, respectively, and the coordinates of the feature point are changed.

Figure 10b shows the step-by-step diagram of the springback of the part during the second step of cutting the edge. The results in Fig. 10b are from numerical simulations. Clamps 2 and 3 are in the unclamped state and clamps 1, 4, 5, and 6 are in the clamped state. The unclamping of clamp 3 at sections B-B leads to a considerable rebound of the feature points 1 to 10, which shows a trend of increasing and then gradually becoming smooth in the section. For section D-D, as clamp 1 changed from unclamped to clamped, at this time, the characteristic points 7, 8, 9, and 10 of the cross-section all experienced large negative springback, indicating the more significant influence of each clamp state on the springback of the workpiece.

Figure 10c is a step-by-step diagram of the springback of the part during the cutting of the edge in the third step. The results in Fig. 10c are from numerical simulations.

Currently, clamps 4 and 5 are in the unclamped state, and clamps 1, 2, 3, and 6 are in the clamped state. The characteristic points of sections A-A and B-B near clamps 4 and 5 occurs springback in the opposite direction. The maximum springback value reaches about 1.4 mm, which is beyond the required tolerance range of the workpiece.

Figure 10d shows the step-by-step diagram of the part's springback during the fourth step's cutting process. The results in Fig. 10d are from numerical simulations. Clamps 5 and 6 are in a loose state, and clamps 1, 2, 3, and 4 are in a clamped state. Due to the clamping of the clamps, the springback values on both sections A-A and B-B tend to decrease relative to the previous step, but the springback values at feature point 10 on each section are relatively large.

According to the above description, during laser cutting of the workpiece contour, the change in the clamping state of the clamp leads to further springback changes in the workpiece where springback has already occurred. In addition, the change occurs in real-time during the laser cutting process, mainly in the tendency of the springback of the clamped part to change in the opposite direction when the clamps of the clamped part are released.

Springback during holes cutting

Figure 11 shows the springback distribution during laser cutting holes. The results in Fig. 11 are from numerical

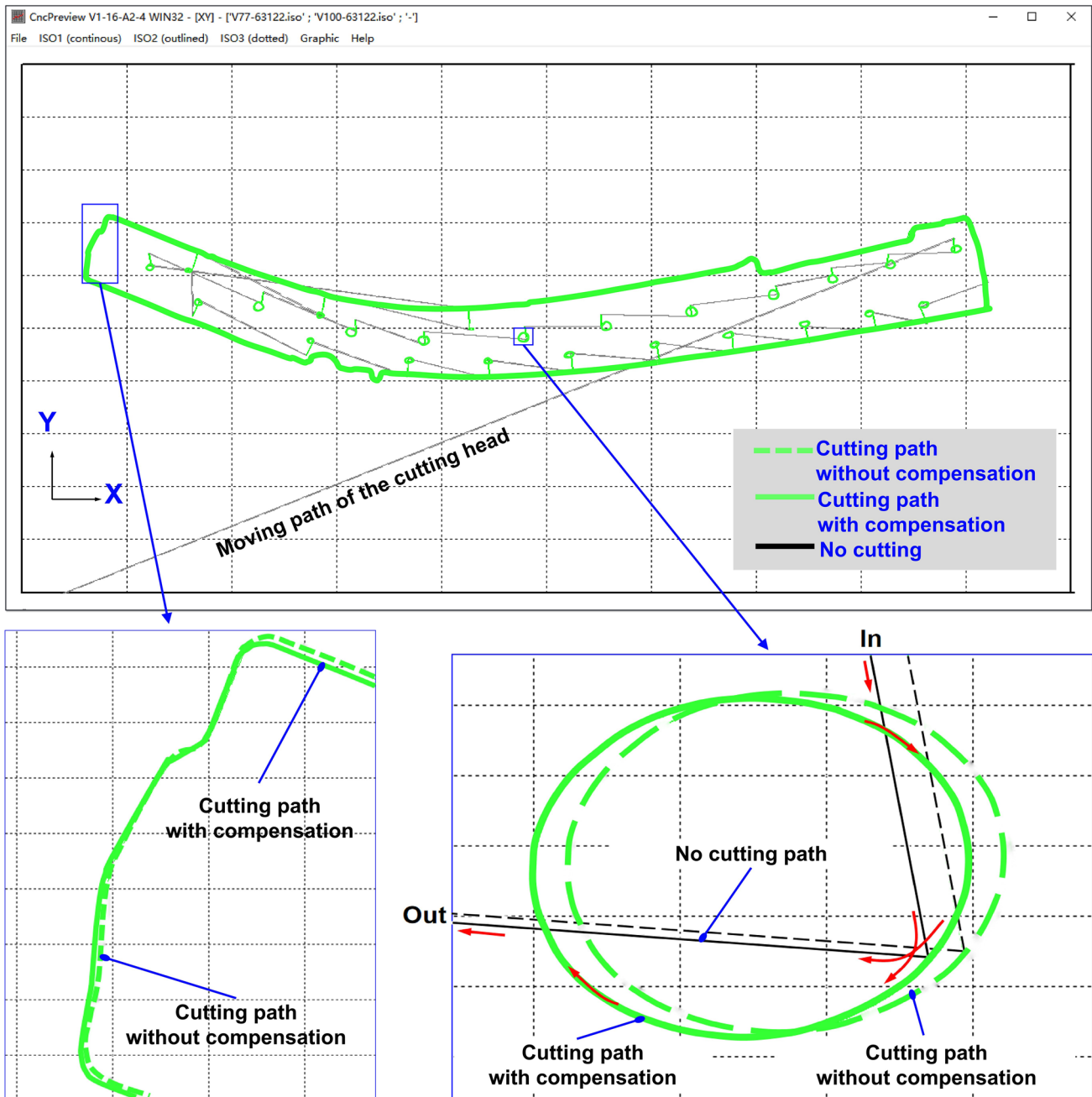


Fig. 14 Cutting paths before and after compensation

simulations. During laser cutting of the holes, all clamps were closed. The last closed clamps 5 and 6 resulted in a reverse distribution of springback values at the characteristic points on cross-sections C–C and D–D. The variation of springback on cross-section A–A and cross-section B–B is relatively small. This laser cutting step is the last cutting process, and the springback at this point determines the accuracy of the part machined throughout the process. Once the part is placed on the inspection tool for passing inspection, it is sent to the following process. However, it is clear

that this part's springback values on sections C–C and D–D have exceeded the allowed tolerances.

Laser cutting path compensation

Due to the springback of the part, the cutting path of the part is changed. The conventional cutting process usually ignores the changed cutting path. Hence, the path of each segment should be compensated separately in reverse according to the springback values. In the laser cutting

Fig. 15 A-pillar 3D laser cutting parts and inspection tools

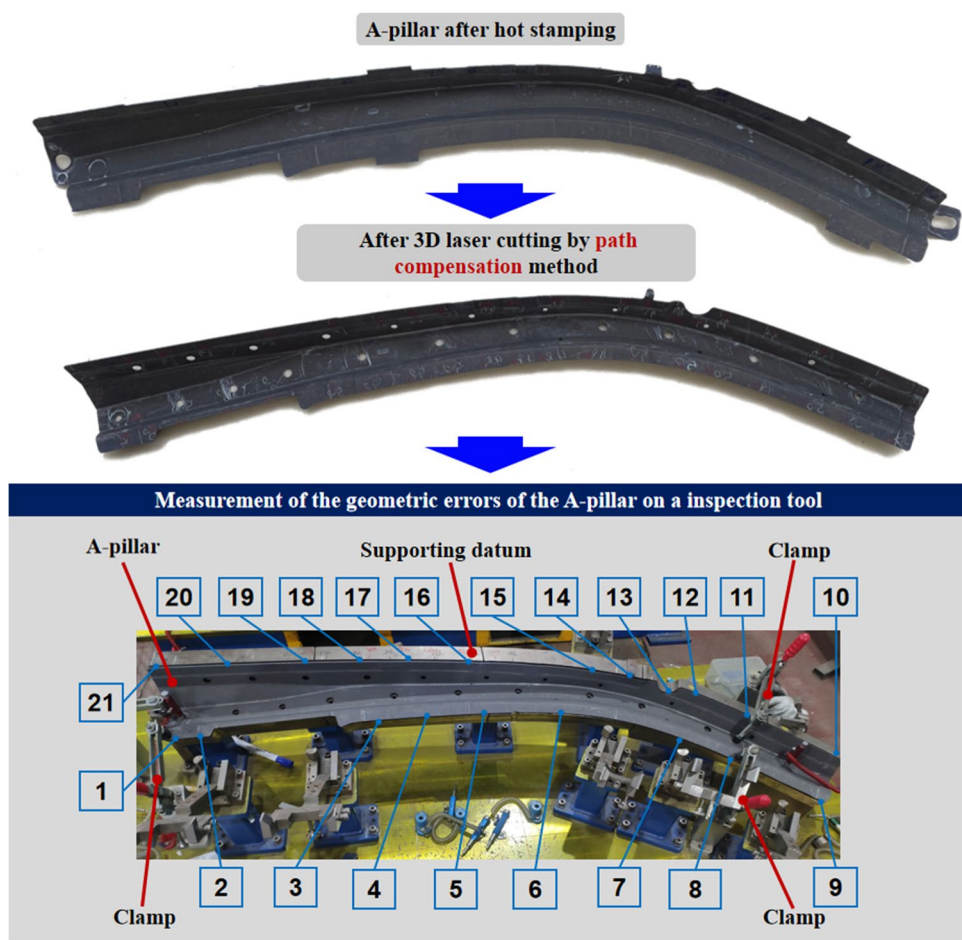


Table 3 Measured values of tracking points on the contour

Tracking point	Tolerance/mm	Measured value/mm	Tracking point	Tolerance/mm	Measured value/mm
T01	(+0.2, -0.8)	-0.18	T12	(+0.2, -0.8)	-0.17
T02	(+0.2, -0.8)	-0.22	T13	(+0.2, -0.8)	0.20
T03	(+0.2, -0.8)	-0.25	T14	(+0.2, -0.8)	-0.18
T04	(+0.2, -0.8)	-0.09	T15	(+0.2, -0.8)	0.20
T05	(+0.2, -0.8)	-0.06	T16	(+0.2, -0.8)	-0.23
T06	(+0.2, -0.8)	-0.14	T17	(+0.2, -0.8)	-0.65
T07	(+0.2, -0.8)	-0.07	T18	(+0.2, -0.8)	0.14
T08	(+0.2, -0.8)	0.15	T19	(+0.2, -0.8)	0.15
T09	(+0.2, -0.8)	-0.02	T20	(+0.2, -0.8)	-0.45
T10	(+0.2, -0.8)	-0.07	T21	(+0.2, -0.8)	0.49
T11	(+0.2, -0.8)	0.05			

process, the contours of the workpiece are processed as straight lines, circular arcs and other features. Each feature has specific position coordinates for its position in 3D space. The position coordinates can be modified in the path code and the path before and after the modification can be previewed in the CncPreview software.

As shown in Fig. 12, a circular hole cutting process is used to describe the path compensation method by combining the of numerical results. First, after obtaining the springback values for each feature point at each step, the springback components can be obtained specifically for each direction, and each component is easily obtained in the numerical simulation. The magnitude and direction of

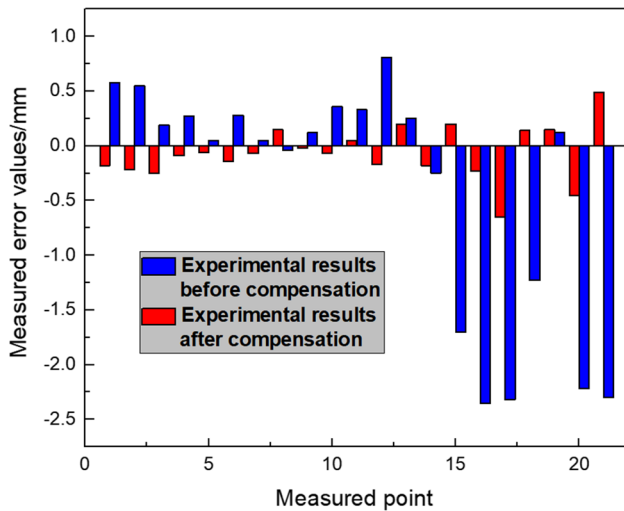


Fig. 16 Contrast of measured error values

each feature point is then added to the original coordinates in the original code. For example, for a straight line determined at two points, when the first coordinate point is modified but not the second, then the path of the line is changed. When the cut is a circular arc or circle, then we change the coordinates of the centre of the circle. In these ways, the compensation can be imported into the curve.

The components of each coordinate axis direction in the 3D software will be imported into the cutting path software CNCPreview for adjustment. The results of the numerical simulation are used to modify the results generated according to the standard 3D model. Follow the above process to compensate for unqualified contour and get the best 3D cutting path, as shown in Fig. 13. The comparison of the contour before and after compensation in the xy-coordinate plane is shown in Fig. 14. The compensated path is imported into the 3D laser cutting machine for cutting process operation.

Experimental verification

As shown in Fig. 15, after obtaining the laser cutting path by the method mentioned above, the laser cutting experiment is carried out on the workpiece after hot stamping. Then the workpiece is put on the designed checker for inspection. Among them, the checker mainly consists of a support table, a clamp, and a related ruler to measure the dimensional deviation of the workpiece. The locations of the 21 points being measured are shown by the serial numbers.

The contour errors measured on the inspection tool are shown in Table 3, and Fig. 16 compares of the measured errors after compensation and the errors without compensation. These results are from experiments. After compensation, it is found that the error of each profile and contour can

be limited to a greater extent within the tolerance range and meet the accuracy requirements. The compensated 3D laser cutting experiment verifies the effectiveness of the above springback compensation method. The novel compensation method effectively improves the 3D laser cutting accuracy, reduces the debugging time, and improves the production efficiency.

After the hot stamping process forms the workpiece, a certain amount of springback has occurred. The springback causes a specific deviation between the semi-finished parts and the 3D digital model, leading to the 3D laser cutting path deviation. In the process of 3D laser cutting, due to the change of clamping force and stress release caused by material removal, the parts will produce further rebound changes, resulting in further deviation of the 3D laser cutting path. The cutting experiment is conducted by compensating for the 3D laser cutting path. The experiment results show that the compensation method proposed in this paper can effectively reduce the contour and profile errors caused by springback.

Conclusions

In this work, a novel process based on improving 3D laser cutting accuracy is proposed for the problem of reduced laser cutting accuracy due to the springback. The cutting path is compensated by the 3D laser cutting single path compensation method considering springback transfer, and the following main conclusions are obtained through numerical simulation and experimental verification.

- 1 A full-process springback simulation model for hot stamping and 3D laser cutting of the A-pillar was established. The hot stamping parts will produce springback due to residual stresses. The clamps have a more significant influence on the springback of the workpiece during the laser cutting process. This is mainly demonstrated by the tendency of the part to springback in the opposite direction of the springback method when the clamp is changed from the clamped state to the unclamped state, which is consistent with the actual process. Therefore, the established springback simulation can effectively predict the overall trend of springback deformation.
- 2 Based on the proposed compensation method of springback, the optimized cutting contour to meet the 3D laser cutting accuracy is obtained. The effectiveness of the compensation method is verified by 3D laser cutting experiment. The contour springback error is reduced by 15%, which effectively improves the 3D laser cutting accuracy of the advanced AHSS part and meets the accuracy requirements.

- 3 In this research, we found that the cutting accuracy can be improved to a certain extent due to laser cutting compensation. That eliminates the need to repeatedly compensate the cutting path or modify the die surface of the hot stamping mold compared to the conventional process. In addition, this compensation method can improve the efficiency of laser cutting of AHSS parts and reduce manufacturing costs. The research can provide theoretical guidance for the practical production of the AHSS part.
- 4 The feasibility of the proposed path compensation method is verified by actual part production. In the future, we will combine machine learning methods to establish a digital and intelligent laser cutting platform to implement prediction and compensation of laser cutting accuracy, reduce manual commissioning cycles and improve production efficiency.

Funding This study was funded by the National Natural Science Foundation of China (grant numbers 52075400, 52275368); Independent Innovation Projects of the Hubei Longzhong Laboratory(2022ZZ-04); the 111 Project (grant number B17034), and the Key Research and Development Program of Hubei Province (grant number 2021BAA200).

Declarations

Conflict of interest We confirm that there are no known conflicts of interest associated with this work.

References

1. Safari H, Nahvi H, Esfahanian M (2017) Improving automotive crashworthiness using advanced high strength steels. *Int J Crashworthines* 23(6):645–659. <https://doi.org/10.1080/13588265.2017.1389624>
2. Wang Z, Lu Q, Cao ZH, Chen H, Huang MX, Wang JF (2022) Review on Hydrogen Embrittlement of Press-hardened Steels for Automotive Applications. *Acta Metall Sinica (English Letters)*. <https://doi.org/10.1007/s40195-022-01408-4>
3. Miraoui I, Boujelbene M, Zaied M (2016) High-Power Laser Cutting of Steel Plates: Heat Affected Zone Analysis. *Adv Mater Sci Eng*. <https://doi.org/10.1155/2016/1242565>
4. Russo Spena P (2017) CO2 Laser Cutting of Hot Stamping Boron Steel Sheets. *Metals-Basel*. <https://doi.org/10.3390/met7110456>
5. Gautam GD, Mishra DR (2019) Dimensional accuracy improvement by parametric optimization in pulsed Nd:YAG laser cutting of Kevlar-29/basalt fiber-reinforced hybrid composites. *J Braz Soc Mech Sci*. <https://doi.org/10.1007/s40430-019-1783-y>
6. Shrivastava PK, Singh B, Shrivastava Y, Pandey AK (2019) Prediction of geometric quality characteristics during laser cutting of Inconel-718 sheet using statistical approach. *J Braz Soc Mech Sci* 41(5). <https://doi.org/10.1007/s40430-019-1727-6>
7. Nguyen V, Altarazi F, Tran T, Hu J (2022) Optimization of Process Parameters for Laser Cutting Process of Stainless Steel 304: A Comparative Analysis and Estimation with Taguchi Method and Response Surface Methodology. *Math Probl Eng* 2022:1–14. <https://doi.org/10.1155/2022/6677586>
8. Madić M, Mladenović S, Gostimirović M, Radovanović M, Janković P (2020) Laser cutting optimization model with constraints: Maximization of material removal rate in CO2 laser cutting of mild steel. *Proc IME B J Eng Manuf*. <https://doi.org/10.1177/0954405420911529>
9. Shrivastava PK, Singh B, Shrivastava Y, Pandey AK, Nandan D (2019) Investigation of optimal process parameters for laser cutting of Inconel-718 sheet. *Proc Inst Mech Eng C J Mech Eng Sci*. <https://doi.org/10.1177/0954406219895533>
10. Girdu CC, Gheorghie C, Radulescu C, Cirtina D (2021) Influence of Process Parameters on Cutting Width in CO2 Laser Processing of Hardox 400 Steel. *Applied Sciences* 11(13). <https://doi.org/10.3390/app11135998>
11. Jadhav A, Kumar S (2019) Laser cutting of AISI 304 material: an experimental investigation on surface roughness. *Adv Mater Process Technol* 5(3):429–437. <https://doi.org/10.1080/2374068x.2019.1622297>
12. Buj-Corral I, Costa-Herrero L, Dominguez-Fernandez A (2021) Effect of Process Parameters on the Quality of Laser-Cut Stainless Steel Thin Plates. *Metals-Basel* 11(8). <https://doi.org/10.3390/met11081224>
13. Ninikas K, Kechagias J, Salonitis K (2021) The Impact of Process Parameters on Surface Roughness and Dimensional Accuracy during CO2 Laser Cutting of PMMA Thin Sheets. *J Manuf Mater Process*. <https://doi.org/10.3390/jmmp5030074>
14. Lazov L, Nikolić V, Jovic S, Milovančević M, Deneva H, Teirumenieka E, Arsic N (2018) Evaluation of laser cutting process with auxiliary gas pressure by soft computing approach. *Infrared Phys Technol*. <https://doi.org/10.1016/j.infrared.2018.04.007>
15. Nabavi SF, Farshidianfar MH, Farshidianfar A, Marandi S (2022) Dross formation modeling in the laser beam cutting process using energy-based and gas-based parameters. *Int J Adv Manuf Technol*. <https://doi.org/10.1007/s00170-022-09019-0>
16. Chaki S, Bathe RN, Ghosal S, Padmanabham G (2018) Multi-objective optimisation of pulsed Nd:YAG laser cutting process using integrated ANN-NSGAI model. *J Intell Manuf* 29(1):175–190. <https://doi.org/10.1007/s10845-015-1100-2>
17. Rohman MN, Ho JR, Tung PC, Lin CT, Lin CK (2022) Prediction and optimization of dross formation in laser cutting of electrical steel sheet in different environments. *J Market Res*. <https://doi.org/10.1016/j.jmrt.2022.03.106>
18. Shin JS, Oh SY, Park H, Chung CM, Seon S, Kim TS, Lee L, Choi B-S, Moon J-K (2017) High-speed fiber laser cutting of thick stainless steel for dismantling tasks. *Opt Laser Technol*. <https://doi.org/10.1016/j.optlastec.2017.03.040>
19. Oh SY, Shin JS, Kim TS, Park H, Lee L, Chung CM, Lee J (2019) Effect of nozzle types on the laser cutting performance for 60-mm-thick stainless steel. *Opt Laser Technol*. <https://doi.org/10.1016/j.optlastec.2019.105607>
20. Rodrigues GC, Levichev N, Vorkov V, Duflou JR (2019) Thickness validation of modeling tools for laser cutting applications. *Procedia Manufacturing*. <https://doi.org/10.1016/j.promfg.2019.02.152>
21. Shin JS, Oh SY, Park SK, Park H, Lee J (2021) Improved underwater laser cutting of thick steel plates through initial oblique cutting. *Opt Laser Technol*. <https://doi.org/10.1016/j.optlastec.2021.107120>
22. Jiang HJ, Ren YX, Lian JW, Xu WL, Gao NH, Wang X-G, Jia C-S (2022) A new predicting model study on U-shaped stamping springback behavior subjected to steady-state temperature field. *J Manuf Process* 76:21–33. <https://doi.org/10.1016/j.jmapro.2022.02.004>

23. Lajarin SF, Filho RAC, Rebeyka CJ, Nikhare CP, Marcondes PVP (2020) Numerical study on variation of chord modulus on the springback of high-strength steels. *Int J Adv Manuf Technol* 106(11–12):4707–4713. <https://doi.org/10.1007/s00170-020-04975-x>
24. Gautam V, Kumar DR (2018) Experimental and numerical investigations on springback in V-bending of tailor-welded blanks of interstitial free steel. *P I Mech Eng B-J Eng* 232(12):2178–2191. <https://doi.org/10.1177/0954405416687146>
25. Wang Z, Hu Q, Yan J, Chen J (2016) Springback prediction and compensation for the third generation of UHSS stamping based on a new kinematic hardening model and inertia relief approach. *Int J Adv Manuf Technol* 90(1–4):875–885. <https://doi.org/10.1007/s00170-016-9439-x>
26. Dang VT, Labergère C, Lafon P (2018) Adaptive metamodel-assisted shape optimization for springback in metal forming processes. *Int J Mater Form* 12(4):535–552. <https://doi.org/10.1007/s12289-018-1433-4>
27. Lin J, Hou Y, Min J, Tang H, Carsley JE, Stoughton TB (2019) Effect of constitutive model on springback prediction of MP980 and AA6022-T4. *Int J Mater Form* 13(1):1–13. <https://doi.org/10.1007/s12289-018-01468-x>
28. Li B, Melkote SN (2001) Fixture Clamping Force Optimisation and its Impact on Workpiece Location Accuracy. *Int J Adv Manuf Technol*. <https://doi.org/10.1007/s001700170198>
29. Abedini V, Shakeri M, Siahmargouei MH, Baseri H (2014) Analysis of the influence of machining fixture layout on the workpiece's dimensional accuracy using genetic algorithm. *Proc IME B J Eng Manuf*. <https://doi.org/10.1177/0954405413519605>
30. Kang J, Chunzheng D, Jinxing K, Yi C, Yuwen S, Shanglin W (2020) Prediction of clamping deformation in vacuum fixture–workpiece system for low-rigidity thin-walled precision parts using finite element method. *Int J Adv Manuf Technol*. <https://doi.org/10.1007/s00170-020-05745-5>
31. Dingqiang P, Liming W, Chris KM, Yimin S (2021) Position prediction and error compensation for a large thin-walled box-shaped workpiece in a fixture. *Int J Adv Manuf Technol*. <https://doi.org/10.1007/s00170-021-07632-z>
32. Huang HL, Jywe WY, Cho MC (2015) Development of a simple laser-based 2D contouring accuracy compensation system for the laser cutting machine. *Optik*. <https://doi.org/10.1016/j.ijleo.2015.08.244>

Publisher's note Springer Nature remains neutral with regard to jurisdictional claims in published maps and institutional affiliations.

Springer Nature or its licensor (e.g. a society or other partner) holds exclusive rights to this article under a publishing agreement with the author(s) or other rightsholder(s); author self-archiving of the accepted manuscript version of this article is solely governed by the terms of such publishing agreement and applicable law.